

Hydrogen Bonding and Chain Conformational Isomerization of Alcohols Probed by Ultrasonic Absorption and Shear Impedance Spectrometry

R. Behrends and U. Kaatz*
 Drittes Physikalisches Institut, Georg-August-Universität, Bürgerstrasse 42-44, D-37073 Göttingen, Germany

Received: January 30, 2001; In Final Form: March 26, 2001

The acoustical absorption spectra between 300 kHz and 3 GHz and the complex shear viscosity spectra between 6 and 120 MHz for some monohydric alcohols are reported. The acoustical spectra exhibit two relaxation regions, one located at frequencies around some hundred MHz and the other one around some GHz. The shear viscosity spectra reveal a relaxation process in conformity with the low-frequency acoustical relaxation. This relaxation is assigned to fluctuations in the structure of hydrogen bonded alcohol clusters. The high-frequency acoustical relaxation is discussed in terms of a damped torsional oscillator model of alkyl chain isomerization, corresponding with the rotational isomerization of *n*-alkanes. The high frequency (>5 GHz) shear viscosity of the alcohols is estimated and found in the same order (1 mPa s) as that for *n*-alkanes.

1. Introduction

The properties of alcohols are subject of considerable scientific interest, not only because of their widespread use as solvents in chemical engineering and in the pharmaceutical industry. The multitude of fascinating features of alcohols, reflecting simultaneously present effects from hydrogen bonding and van der Waals interactions, have stimulated many theoretical and experimental studies. Favorable conditions are offered for such studies by the alcohols, which display a great variability in the numbers of hydrogen bonding and hydrocarbon groups per molecule. In addition, a variety of steric isomers exists for many alcohols, resulting in a variety of different liquid structures, as indicated, for instance, by significant differences in the static electric permittivity.¹ Another favorable characteristic of alcohols is their ability to form, over broad ranges of composition and temperature, mixtures with water and with hydrophobic liquids as well. Many experimental techniques have been applied in the past to elucidate the properties of alcohols and of their mixtures. Though the viscosity reflects the intermolecular interactions of a fluid in an obvious but collective manner, only recently attention has been directed toward the viscoelastic properties of alcohols, particularly in view of glass forming features.²

The viscoelastic behavior of fluids is frequently used to characterize colloidal interactions among the particles in dispersions and emulsions, including micellar systems and vesicle solutions.³ Due to the comparatively large particle size, relaxation characteristics in the viscosity of those systems are often studied using commercially available low-frequency viscometers. Here the attempt is made to observe viscosity relaxations at MHz and GHz frequencies utilizing two methods, ultrasonic absorption spectrometry (300 kHz to 3 GHz) and shear impedance spectrometry (6–120 MHz). Both methods are complementary to depolarized Brillouin light scattering experiments.^{4,5} Results for some monohydric alcohols are compared to recent spectra for *n*-alkanes.⁶

2. Experimental Section

Alcohols. We measured the four unbranched normal alcohols: 1-hexanol (Merck, >98%), 1-octanol (Fluka, ≥99.5%),

TABLE 1: Experimental Errors of the Acoustical Absorption Coefficient and Shear Viscosity Data

ν , MHz	$\Delta\alpha/\alpha$	ν , MHz	$\Delta\eta'_s/\eta'_s$	$\Delta\eta''_s/\eta''_s$
0.3–1	0.1	6–10	0.1	0.2
1–20	0.05	10–20	0.05	0.1
20–40	0.03	20–60	0.03	0.06
40–300	0.01	60–80	0.05	0.1
300–3000	0.02	80–120	0.1	0.2

1-decanol (Merck, >99%), and 1-dodecanol (Merck, >98%), as well as the four branched monohydric alcohols 3-hexanol (Fluka, ≥98%), 2-methyl-1-pentanol (Fluka, >99%), 2-ethyl-1-hexanol (Fluka, >99%), and 3,7-dimethyl-1-octanol (Fluka, ≥98%).

All alcohols were used without additional purification. Measurements were performed at 25 °C and with 1-octanol also at 15 °C and 20 °C. The density ρ of the liquids (Table 3) has been determined picnometrically. The static shear viscosity $\eta_{so} = \eta(\nu \rightarrow 0)$ (Table 3) has been measured using a falling ball viscometer (Haake B/BH) and for some alcohols also with the aid of Ubbelohde-type capillary viscometers (Schott, KPG).

Acoustical Absorption Spectrometry. For nonmetallic liquids, for which contributions from the heat conductivity can be neglected, the asymptotic high-frequency absorption coefficient

$$\alpha_{asy} = \lim_{\nu \rightarrow \infty} \alpha(\nu) \quad (1)$$

of longitudinal compressional (ultrasonic) waves is given by

$$\alpha_{asy} = \frac{8\pi^2\nu^2}{3\rho c^3} \left(\eta_s(\nu) + \frac{3}{4}\eta_v(\nu) \right) \quad (2)$$

Here ν denotes the frequency of the sonic wave, α is the absorption coefficient, and c is the sound velocity of the liquid. The so-called volume viscosity η_v is related to the curl-free part of the acoustical field. Hence, if no additional processes contribute in excess to α_{asy} to the absorption coefficient $\alpha(\nu)$, acoustical absorption spectrometry enables the frequency dependence of the quantity $\eta_s + (3/4)\eta_v$ to be measured. On

TABLE 2: Sound Velocity c and Parameters of the Relaxation Spectral Function (Equation 10) Representing the Ultrasonic Absorption Spectra of the Monohydric Alcohols at the Temperature T

alcohol	$T, ^\circ\text{C}$	$c, \text{m/s} \pm 0.5\%$	$A_{\alpha 1}, 10^{-3} \pm 10\%$	$\tau_{\alpha 1}, \text{ns} \pm 10\%$	$A_{\alpha 2}, 10^{-3} \pm 10\%$	$\tau_{\alpha 2}, \text{ps} \pm 20\%$	$B, \text{ps} \pm 5\%$
1-hexanol	25	1302	19	0.27	110	73	64
3-hexanol	25	1253	23	0.97	99	247	105
2-methyl-1-pentanol	25	1275	13	0.86	108	133	88
1-octanol	15	1390	36	0.43	90	100	108
	20	1365	33	0.41	85	92	100
	25	1339	33	0.38	73	92	97
2-ethyl-1-hexanol	25	1320	30	0.82	159	118	97
1-decanol	25	1380	28	0.66	114	99	112
3,7-dimethyl-1-octanol	25	1332	55	0.55	245	68	110
1-dodecanol	25	1402	20	1.43	193	107	117

TABLE 3: Density ρ , Static Shear Viscosity^a η_{so} , and Parameters of the Relaxation Spectral Function (Equations 11 and 12) Describing the Frequency Dependent Shear Viscosity Data for the Monohydric Alcohols at 25 °C^b

alcohol	$\rho, \text{mg/cm}^3 \pm 0.2\%$	$\eta_{so}, \text{mPa} \cdot \text{s} \pm 2\%$	$\eta_s(\infty), \text{mPa} \cdot \text{s} \pm 5\%$	$A_s, \text{mPa} \cdot \text{s} \pm 20\%$	$\eta_s(0), \text{mPa} \cdot \text{s} \pm 5\%$	τ_s, ns
1-hexanol	881.0	4.65	3.3	1.1	4.4	0.27
3-hexanol	814.4	4.64	4.1	0.3	4.4	0.97
2-methyl-1-pentanol	817.3	5.53	4.6	0.7	5.3	0.86
1-octanol	824.0	7.63	4.3	3.1	7.4	0.38
2-ethyl-1-hexanol	828.0	7.87	6.7	1.0	7.7	0.82
1-decanol	829.0	10.97	4.9	6.2	11.1	0.66
3,7-dimethyl-1-octanol	826.0	11.14	6.5	5.2	11.7	0.55
1-dodecanol	834.0	17.04	7.7	8.5	16.2	1.43

^a The η_{so} values are weighted means of the data measured with the falling ball viscometer and the capillary viscometer. ^b The relaxation time τ_s has been fixed at the relaxation time $\tau_{\alpha 1}$ of the low-frequency ultrasonic relaxation process (Table 2).

favorable conditions, the contributions from the shear viscosity and from the volume viscosity can even be separated from one another.

Because of the strong frequency dependence of the absorption coefficient α (eq 2) different methods of measurements are required to cover the frequency range from 0.3 to 3000 MHz.⁹ At $\nu < 15$ MHz, the quality factor of cavity resonator cells filled with the sample has been determined relative to a suitably chosen reference liquid. We used two different resonators, each specially matched to a frequency range.^{10,11} At $\nu > 20$ MHz, a variable path length pulse-modulated wave transmission method has been applied for the direct (absolute) determination of the absorption coefficient. Three different cells^{12,13} have been utilized, each cell again matched to a particular frequency range. The cells mainly differed from one another by the principles of piezoelectric transducer operation and by details in the realization of the sample length variation.

Shear Wave Impedance Spectrometry. The complex shear wave impedance

$$(i^2 = -1)$$

$$Z_s(\nu) = Z'_s(\nu) + iZ''_s(\nu) \quad (3)$$

is related to the shear viscosity and density of a liquid as

$$Z_s(\nu) = (2\pi i \rho \nu \eta_s(\nu))^{1/2} \quad (4)$$

Hence, measurements of Z_s as a function of frequency allow for the determination of the frequency dependent complex shear viscosity

$$\eta_s(\nu) = \eta'_s(\nu) - i\eta''_s(\nu) \quad (5)$$

of a liquid. In this notation, the real part $\eta'_s(\nu)$ of the shear viscosity represents the irreversible viscous molecular processes whereas the imaginary part $-\eta''_s(\nu)$ considers the reversible elastic mechanisms. Such mechanisms may become obvious at high frequencies, when the shearing stress oscillates so rapidly that the time of application of stress is too small to allow the molecules to completely re-adjust their relative positions.¹⁴ Even

when exhibiting non-Newtonian viscoelastic behavior, however, the penetration depth for shear waves in low-viscosity liquids is small. Therefore, we again applied resonator techniques in order to reach a sufficiently high sensitivity in the measurements.¹⁵ Basically, the resonance frequency and quality factor for modes of AT-quartz cells have been measured sensitively. These quantities yield the complex $Z_s(\nu)$ from which $\eta_s(\nu)$ follows according to eq 4. We used two AT-quartz resonator cells, one favorably operated at frequencies between 6 and 20 MHz, the other one between 20 and 120 MHz.¹⁵

Sound Velocity Measurements. The sound velocity c of the alcohols has been obtained as a byproduct of the acoustical absorption spectrometry. In the lower part of the measuring range ($\nu < 15$ MHz), c has been derived from the series of resonance frequencies of the cavity resonators.^{9,10} At higher frequencies ($\nu > 20$ MHz) c followed from the waviness in the transfer function of the respective variable path length cells, resulting from multiple reflections of the sonic signal at the liquid/transducer interfaces.

Experimental Errors. The temperature T of all specimen cells was controlled to within ± 0.05 K and was measured with an accuracy of ± 0.02 K. Errors from temperature fluctuations of the samples therefore were small. The relative experimental error $\Delta\rho/\rho$ in the density measurements was smaller than ± 0.002 . Repeated measurements of the viscosity of the liquids using two different balls in the falling ball viscometer and also comparison of these results to those from the capillary viscometers showed the static viscosity accurate to within $\Delta\eta_{so}/\eta_{so} = \pm 0.02$.

In the acoustical absorption coefficient, sound velocity, and shear impedance measurements synthesized signal generators have been used throughout so that frequency fluctuations can be neglected. In the ultrasonic resonator measurements ($\nu < 15$ MHz) the main source of small errors are possible disturbances in the cell geometry when the sample is exchanged for the reference liquid. These errors, depending upon the absorption coefficient to be determined, have been estimated from repeated measurements, always emptying, cleaning, and refilling the cells between two runs. In the lower measuring range of the variable

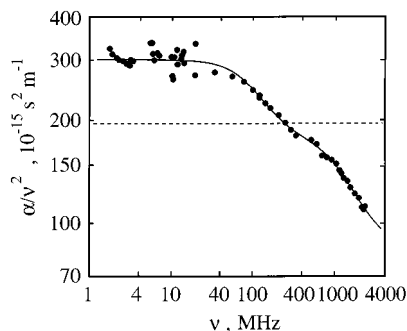


Figure 1. Frequency normalized plot of the ultrasonic absorption spectrum of 1-dodecanol at 25 °C. The full curve is the graph of a spectral function with two relaxation terms. The dashed line indicates the $\alpha\nu^2$ value which according to eq 7 would follow from a frequency independent shear viscosity.

path length method ($\nu < 40$ MHz) diffraction losses due to the finite diameter of the piezoelectric transducers have to be taken into account by calibration measurements,¹⁶ leading to a somewhat less favorable accuracy than at higher frequencies (Table 1).

Within the frequency range under consideration the dispersion in the sound velocity of the alcohols is small and is thus omitted in this study. The c values measured at different frequencies agree to within $\Delta c/c = \pm 0.005$.

The accuracy of the new shear impedance spectrometer has been estimated from the overlap of data obtained from the two different AT-quartz resonators, from measurements of reference liquids, like water or *n*-dodecane, with well-known static viscosity η_{so} for which no relaxation is expected in the relevant frequency range, and also from repeated measurements of the alcohols. Since the latter procedure included cleaning and refilling of the cells, it guarantees errors from an incomplete wetting of the shear transducers surfaces not to remain unnoticed. The experimental uncertainties in the complex shear viscosity data are also presented in Table 1.

Regression Analysis of Spectra. In the following discussion, to obtain the values for the parameters P_j , $j = 1, \dots, J$, the measured spectra $S(\nu_n)$, either acoustic absorption or shear viscosity, will be analytically described by relaxation spectral functions $R(\nu_n, P_j)$. For this purpose a Marquardt algorithm¹⁷ is used that minimizes the reduced variance

$$\chi^2(P_1, \dots, P_j) = \frac{1}{N-J-1} \sum_{n=1}^N \left(\frac{S(\nu_n) - R(\nu_n, P_j)}{\Delta S(\nu_n)} \right)^2 \quad (6)$$

Here ν_n , $n = 1, \dots, N$ are the frequencies of measurements, and the inverse experimental errors $\Delta S^{-1}(\nu_n)$ of S at ν_n are used as weighing factors in eq 6.

3. Results

Ultrasonic Absorption Spectra. In Figure 1 the acoustical absorption spectrum for 1-dodecanol at 25 °C is shown in the format $\alpha\nu^2$ vs ν . For a liquid without ultrasonic relaxation process a constant $\alpha\nu^2$ value is expected which, according to eq 2 is given by a frequency-independent shear and volume viscosity. The frequency normalized sonic absorption spectrum for 1-dodecanol, however, exhibits two dispersion regions ($d(\alpha/\nu^2)/d\nu < 0$) within our measuring range. One dispersion occurs at frequencies around some hundred MHz, the other one around some GHz. Hence the acoustical absorption coefficient of the alcohol clearly reflects two distinct relaxation processes. Interesting, even due to the low-frequency dispersion the α/ν^2

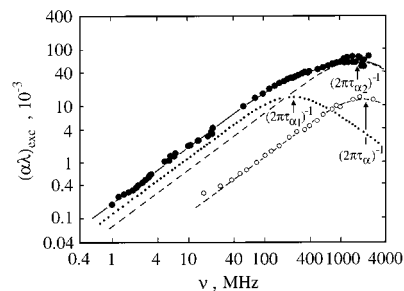


Figure 2. Ultrasonic excess absorption spectrum for 1-dodecanol (full symbols) and *n*-dodecane (open symbols) at 25 °C. The full curve represents the spectral function with two relaxation terms defined by eq 10. The subdivision of this function into a low-frequency term (“ α_1 ”) and a high-frequency term (“ α_2 ”) is indicated by dotted and dashed curves, respectively. The dodecane spectrum is described by one relaxation term with discrete relaxation time ($A_{\alpha_1} = 0$, $\tau_{\alpha_2} = \tau_\alpha$ in eq 10).

data become smaller than the contribution

$$\left(\frac{\alpha}{\nu^2} \right)_{\eta_{so}} = \frac{8\pi^2}{3\rho c^3} \eta_{so} \quad (7)$$

from the static shear viscosity η_{so} to the sonic absorption. This is the first clear indication of both the shear viscosity and the volume viscosity of the alcohol to be subject to relaxation characteristics in the ultra- and hypersonic frequency range.

To accentuate the high-frequency part of the spectrum, in Figure 2 the acoustic absorption data are displayed in the format $(\alpha\lambda)_{exc}$ vs ν . Here $\lambda = c/\nu$ is the sonic wavelength within the liquid. The suffix “exc” indicates that only the part of the total absorption per wavelength $\alpha\lambda$ is shown that exceeds the background contribution

$$(\alpha\lambda)_{bg} = B\nu \quad (8)$$

with B independent of frequency. In the frequency normalized representation of data (Figure 1) the background contribution is simply a constant value

$$B' = B/c \quad (9)$$

Also presented in Figure 2 is the excess absorption spectrum for *n*-dodecane at 25 °C. Obviously, the hypersonic relaxation of the alcohol with relaxation frequency $\nu_{\alpha_2} = (2\pi\tau_{\alpha_2})^{-1}$ at some GHz corresponds with the ultrasonic relaxation of the alkane, the relaxation frequency $\nu_\alpha = (2\pi\tau_\alpha)^{-1}$ of which is only slightly higher than ν_{α_2} .

In correspondence with the α/ν^2 vs ν plot in Figure 1 the excess absorption spectrum of the alcohol also reveals the second relaxation process with relaxation frequency $\nu_{\alpha_1} = (2\pi\tau_{\alpha_1})^{-1}$ smaller than ν_{α_2} . Since these two relaxation processes are characteristic for all studied alcohols, we used the relaxation spectral function

$$R_\alpha(\nu) = A_{\alpha_1} \frac{\omega\tau_{\alpha_1}}{1 + (\omega\tau_{\alpha_1})^2} + A_{\alpha_2} \frac{\omega\tau_{\alpha_2}}{1 + (\omega\tau_{\alpha_2})^2} + B\nu \quad (10)$$

to represent the measured spectra. In this relation $\omega = 2\pi\nu$ is the angular frequency and A_{α_1} and A_{α_2} are the relaxation amplitudes of the relaxation processes with discrete relaxation times τ_{α_1} and τ_{α_2} , respectively. The values for the parameters of eq 10, as resulting from the nonlinear least-squares regression analysis of the measured ultrasonic absorption spectra, are collected in Table 2.

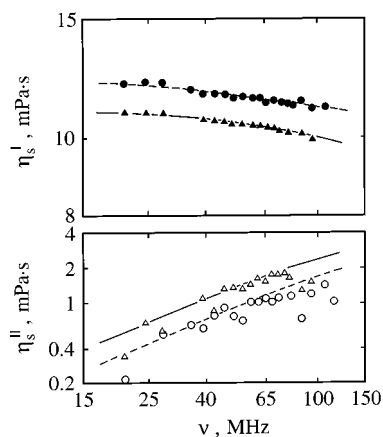


Figure 3. Real part η'_s (full symbols) and negative imaginary part η''_s (open symbols) of the complex shear viscosity displayed as a function of frequency ν for 1-dodecanol (triangles) and 3,7-dimethyl-1-octanol (points, circles) at 25 °C. The curves are graphs of a relaxation spectral function with discrete relaxation time (eq 11) with the parameter values given in Table 3.

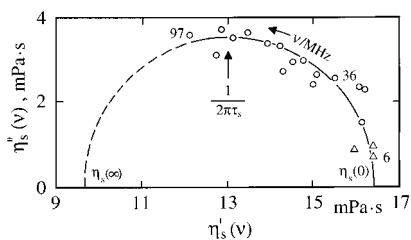


Figure 4. Negative imaginary part η''_s of the shear viscosity shown as a function of the real part η'_s for 1-dodecanol at 25 °C. Figure symbols indicate data from the different AT-quartz resonator cells. The drawn semicircular arc with its center on the η'_s axis is a plot of $R'_s = A_s \omega \tau_s / (1 + \omega^2 \tau_s^2)$ versus $R'_s = \eta'_s(\infty) + A_s / (1 + \omega^2 \tau_s^2)$ with the parameter values as found by the regression analysis of the measured shear viscosity data (Table 3).

Shear Viscosity Spectra. For two alcohols the complex shear viscosity $\eta_s(\nu)$ as resulting from the shear impedance measurements is displayed as a function of frequency in Figure 3. For both alcohols the real part $\eta'_s(\nu)$ decreases with ν . The reduction in the $\eta'_s(\nu)$ values amounts to about 10% within the measuring frequency range, thus slightly exceeding the error in the frequency dependent viscosity data. In correspondence with the dispersion ($d\eta'_s(\nu)/d\nu < 0$) in the real part of the viscosity, however, there exist nonvanishing $\eta''_s(\nu)$ values which increase with ν . This is a strong indication of a shear viscosity relaxation with relaxation frequency $\nu_s = (2\pi\tau_s)^{-1}$ above the available measuring range.

The relaxation characteristics in the shear viscosity are more suggestively displayed by the complex plain representation of $\eta_s(\nu)$ data in Figure 4. Also shown in that diagram is a semicircular arc as the graphical representation¹⁸ of a relaxation process with discrete relaxation time.¹⁹ This arc fits to the data within the limits of experimental error. We thus analyzed the measured shear viscosity spectra in terms of the relaxation spectral function

$$R_s(\nu) = \eta_s(\infty) + \frac{A_s}{1 + i\omega\tau_s} \quad (11)$$

where $\eta_s(\infty)$ is the extrapolated high-frequency shear viscosity (Figure 4) and

$$A_s = \eta_s(0) - \eta_s(\infty) \quad (12)$$

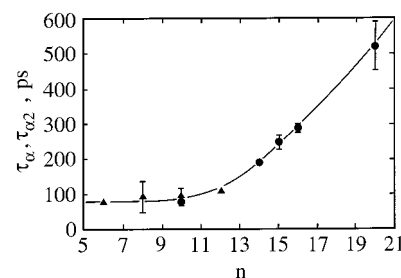


Figure 5. Relaxation times of the high-frequency acoustical relaxation process of the unbranched alcohols ($\tau_{\alpha 2}$, $\text{CH}_3(\text{CH}_2)_{n-1}\text{OH}$, triangles) and of the ultrasonic relaxation of n -alkanes ($\tau_{\alpha 2}$, $\text{CH}_3(\text{CH}_2)_{n-2}\text{CH}_3$, points⁶) displayed as a function of the number of carbon atoms per molecule.

is the relaxation amplitude. To reduce the number of unknown parameters in the regression analysis of the measured $\eta_s(\nu)$ spectra we fixed the relaxation time τ_s at the value $\tau_{\alpha 1}$ of the acoustical absorption spectra (Table 2). This restriction of relaxation time values has been already successfully used in the evaluation of shear viscosity spectra of the alkanes.⁶ Here the $\eta_s(0)$ values extrapolated from the frequency dependent shear viscosity data on the assumption of $\tau_s = \tau_{\alpha 1}$ nicely fit to the experimental static viscosities η_{s0} (Table 3), indicating the consistency of data treatment.

4. Discussion

Chain Conformational Isomerization. The finding that the high-frequency acoustical relaxation of 1-dodecanol occurs almost in the same frequency range as the ultrasonic relaxation of n -dodecane (Figure 2) suggests both to reflect the same molecular mechanism. This suggestion is supported by the chain length dependence of the $\tau_{\alpha 2}$ values of the unbranched alcohols, which nicely fits to that of the τ_{α} data of alkanes (Figure 5). It is, therefore, an obvious attempt to discuss the high-frequency ultrasonic relaxation of alcohols in close analogy to the alkanes, thus to evaluate the relaxation parameters in terms of collective modes of alkyl chain isomerization.⁶ This view is confirmed by additional measurements of mixtures of 1-dodecanol with n -tetradecane with mole fraction of the alkane up to 0.5.²⁰ The spectra of the mixtures yield a relaxation time $\tau_{\alpha 2}$ independent of alcohol concentration, thus pointing at a unimolecular chemical equilibrium



between two alcohol conformations A and A^* , with the relaxation rate

$$\tau_{\alpha 2}^{-1} = k_f + k_r \quad (14)$$

given by the forward (k_f) and reverse rate (k_r) constants.

The acoustical relaxation of alkanes had been considered in the light of a coupled torsional oscillator model.^{21–23} Due to the different modes of chain motions this model predicts a series of relaxation terms. We assume the high-frequency relaxation in our spectra to reflect the term with the smallest relaxation frequency, representing the transition from the all-trans conformation of chains to a conformation in which the mean number k of rotated C–C bonds is adopted. The relaxation rate of this first normal mode of coupled torsional oscillators is given by^{21,22}

$$\tau_1^{-1} = 2\nu_{t0} \sin^2\left(\frac{\pi}{2n_{t0}}\right) e^{-\Delta G^\ddagger/RT} \quad (15)$$

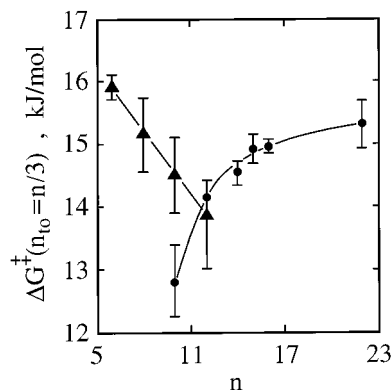


Figure 6. Gibbs free energy of activation ΔG^\ddagger for the first normal mode of coupled torsional oscillations vs number n of carbon atoms per alkyl chain for the unbranched alcohols (triangles) and for some normal alkanes (points⁶). The ΔG^\ddagger values have been derived from eq 15 assuming $\nu_{to} = 8.5$ THz, $n_{to} = n/3$, as well as $\tau_1 = \tau_{\alpha_2}$ (alcohols) and $\tau_1 = \tau_\alpha$ (alkanes). Error bars reflect the uncertainty in the relaxation time data.

where ν_{to} denotes the characteristic frequency for the rotation of an individual C–C bond, n_{to} is the number of individual torsional oscillators per chain, and ΔG^\ddagger is the Gibbs free energy of activation. Using $\nu_{to} = 8.5$ THz as originally reported for ethane²⁴ the ΔG^\ddagger values for n -alkanes have been derived from eq 15 at different n_{to} values.⁶ It was found that the assumption of three carbon atoms in the alkyl chain to form one oscillating unit leads to the best agreement with activation enthalpy and entropy data from temperature-dependent relaxation time measurement. Here the error in the experimental τ_{α_2} data for 1-octanol at three different temperatures is too large to allow for a reliable determination of the activation enthalpy and entropy. For this reason we calculated the Gibbs free energy of activation for the alcohols using $\nu_{to} = 8.5$ THz and $n_{to} = n/3$ as with the alkanes. Reliable ΔG^\ddagger values on the order of 15 kJ/mol have been obtained, indicating the “ α_2 ” term in the ultrasonic absorption spectra of alcohols to in fact reflect the first normal mode of alkyl chain rotational isomerization. For the unbranched alcohols and for the normal alkanes the Gibbs free energies are displayed in Figure 6.

For a unimolecular equilibrium of alcohol isomers (eq 13), the relaxation amplitude, according to

$$A_{\alpha_2} = \frac{\pi \Gamma_2 c_\infty^2 \rho}{RT} \Delta V_{ad,2}^2 \quad (16)$$

is related to the adiabatic reaction volume

$$\Delta V_{ad,2} = \frac{\beta_\infty}{\rho c_{p,\infty}} \Delta H + \Delta V \quad (17)$$

In these equations, Γ_2 is a stoichiometric factor which, for the equilibrium under consideration, is given by

$$\Gamma_2^{-1} = [A]^{-1} + [A^*]^{-1} \quad (18)$$

c_∞ , $c_{p,\infty}$, and β_∞ are the extrapolated high-frequency sound velocity, heat capacity at constant pressure, and thermal expansion coefficient, and ΔH and ΔV are the reaction enthalpy and isothermal reaction volume. Using reasonable reaction enthalpy values on the order of 1 kJ/mol the ΔH term in eq 17 turns out to be small so that $\Delta V_{ad,2} \approx \Delta V$. If ΔV_o denotes the molar change in the adiabatic volume associated with the rotation of a single C–C bond and k the number of rotating

bonds,

$$\Delta V_{ad,2} = k \Delta V_o \quad (19)$$

follows and

$$\Gamma_2 = \frac{k}{n-1} \left(1 - \frac{k}{n-1} \right) \quad (20)$$

Since we know neither k nor ΔV_o , we estimate minimum ΔV_o data, using $k = 0.5(n-1)$, corresponding with $[A] = [A^*]$ and thus with $\Delta H = 0$ and thus using the maximum $\Gamma_2 (=0.25)$. Volume changes ΔV_{omin} between 1.9 cm³/mol and 2.5 cm³/mol result from the A_{α_2} data for the alcohols. These ΔV_{omin} values are quite reasonable in view of $\Delta V_o = 1.8$ cm³/mol for long chain alkanes.²⁵ This is particularly true because the n -alkanes and the unbranched alcohols show somewhat different molar volumes, following the relations

$$V_m = 16.12 \text{ cm}^3/\text{mol}(n-2) + 65.6 \text{ cm}^3/\text{mol} \quad (21)$$

and

$$V_m = 16.64 \text{ cm}^3/\text{mol}(n-1) + 41.4 \text{ cm}^3/\text{mol} \quad (22)$$

derived from the measured densities (Table 3, refs 6 and 20), respectively.

Even though reasonable ΔV_{omin} values result from the A_{α_2} data, the high presupposed degree $k/(n-1) = 0.5$ of rotated C–C bonds might be questioned. This is particularly true since for alkanes, assuming $\Delta V_o = 1.8$ cm³/mol, the more suggestive $k/(n-1)$ values between 0.24 (n -decane) and 0.14 (n -eicosane) had been found.⁶ Alternatively, the A_{α_2} values may be considered to contain contributions from other relaxation mechanisms, unnoticed as separate terms in the spectra due to the location of the “ α_2 ” relaxation at the high-frequency limit of the measuring range.

Single H-Bonded Dipolar Group Reorientation. Dielectric spectra $\epsilon(\nu) = \epsilon'(\nu) - i\epsilon''(\nu)$ of alcohols reveal three relaxation terms,^{26,27} of which the low-frequency one (“d1”) may be subject to a Davidson–Cole relaxation time distribution²⁸ so that the complex (electric) permittivity may be generally represented by the spectral function

$$R_d(\nu) = \epsilon(\infty) + \frac{\Delta A_{d1}}{(1 + i\omega\tau_{d1})^{1-b}} + \frac{\Delta A_{d2}}{1 + i\omega\tau_{d2}} + \frac{\Delta A_{d3}}{1 + i\omega\tau_{d3}} \quad (23)$$

Here b denotes a parameter that measures the width of the (unsymmetrical) relaxation time distribution.²⁹

It is now accepted that the high frequency (“d3”) term, with relaxation frequency $\nu_{d3} = (2\pi\tau_{d3})^{-1}$ far above our measuring range, reflects the rotation of non-hydrogen-bonded OH-groups around the C–O bond. Computer simulation studies of methanol, ethanol, and 1-propanol reveal a content of non-H-bonded monomers of only 1.1–2% of the alcohol molecules at room temperature.³⁰ The other relaxation terms in eq 23 are assigned to reorientational motions of single hydrogen bonded (“d2”) and double H-bonded (“d1”) OH-groups within the chainlike alcohol molecular networks.^{31,32} The content of single H-bonded OH-groups, again taken from computer simulations of methanol,^{33,34} ethanol,^{30,35} and 1-propanol³⁰ is about 15%. Hence, about 80% of the alcohol molecules are double hydrogen bonded.

There are indications of the dielectric relaxations associated with the single and double H-bonded OH-group rotation to be

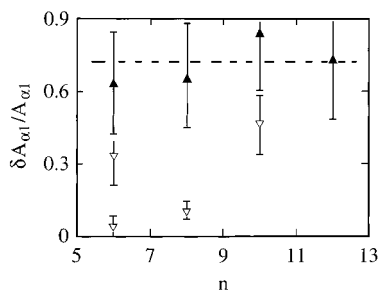


Figure 7. Relaxation amplitude ratio $\delta A_{\alpha 1}/A_{\alpha 1}$ as following from the shear viscosity relaxation (eq 24) for the branched (open symbols) and unbranched (full symbols) monohydric alcohol plotted against the number n of carbon atoms per molecule.

controlled by a wait-and-switch mechanism.^{31,32} The dipolar group will change its orientation preferably if an additional molecule exists in a suitable position that lowers the activation enthalpy for the dipole reorientation and that additionally offers a suitable site for the formation of a new bond.^{36,39} Within the framework of this model of dipole reorientation the dielectric relaxation time is the time for which a hydrogen bonded group has to wait until favorable conditions exist for the reorientation process. The reorientation itself resembles a fast switching.^{38,40} This model of dipole reorientation involves the dielectric relaxations “d1” and “d2” to also reflect translational motions of neighboring molecules, in conformity with the finding that the activation enthalpies from the dielectric relaxation times τ_{d1} and τ_{d2} increase with the length of the alkyl chains of alcohol molecules.³¹ Hence, these molecular mechanisms underlying the dielectric spectra of alcohols may also contribute relaxation characteristics to the acoustic absorption spectra.

For the monohydric alcohols from 1-hexanol to 1-decanol dielectric relaxation times τ_{d2} between 40 ps and 80 ps have been reported.⁴¹ These values are somewhat smaller than the relaxation times $\tau_{\alpha 2}$ of the ultrasonic spectra (Table 2). Obviously, an acoustical relaxation related to the wait-and-switch mechanism of the single H-bonded OH-group reorientation may also contribute to the $A_{\alpha 2}$ values and may thus simulate too large volume changes if the ultrasonic relaxation amplitude is evaluated solely in terms of the alkyl chain isomerization.

Hydrogen Bonded Cluster Fluctuations. The assumption of the low-frequency ultrasonic relaxation process to reflect fluctuations in the structure of the hydrogen bonded chain like alcohol clusters is supported by an almost perfect agreement of the relaxation times $\tau_{\alpha 1}$ of the series of unbranched monohydric alcohols with the corresponding longitudinal dielectric relaxation times $\tau_{d1}\epsilon(\infty)/\epsilon(0)$.^{41,42,43} Here $\epsilon(0) = \epsilon(\infty) + \sum_{i=1}^3 A_{di}$ denotes the static permittivity. Another remarkable fact is the noticeable relaxation amplitude A_s in the shear viscosity of alcohols (Table 3, Figure 8) which significantly exceeds that of the shear viscosity relaxation of alkanes⁶ ($A_s < 2$ mPa s), thus also pointing at an underlying association mechanism rather than an isomerization process.

Despite of its high amplitude A_s , the shear viscosity relaxation of the alcohols only partly accounts for the low-frequency ultrasonic relaxation. According to eq 2, the dispersion in $\eta_s(\nu)$ results in a contribution

$$\delta A_{\alpha 1} = \frac{4\pi A_s}{3\rho c^2 \tau_s} \quad (24)$$

to the acoustical relaxation amplitude $A_{\alpha 1}$. In Figure 7, the $\delta A_{\alpha 1}/A_{\alpha 1}$ ratio is displayed for the monohydric alcohols under consideration. The shear viscosity relaxation of the unbranched

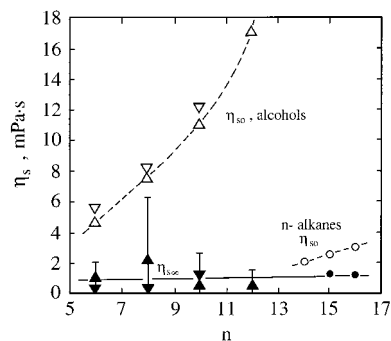


Figure 8. Static shear viscosity η_{so} (open symbols) and shear viscosity η_s (eq 29, closed symbols) at high frequencies ($\nu > 5$ GHz) for unbranched (triangles) and branched (inverse triangles) monohydric alcohols and for some n -alkanes (circles, points), displayed as a function of the number n of carbon atoms per molecule.

alcohols contributes more than 60% to the ultrasonic relaxation amplitude. For the branched alcohols the $\delta A_{\alpha 1}/A_{\alpha 1}$ ratio is distinctly smaller, ranging from 0.04 (3-hexanol) to 0.49 (3,7-dimethyl-1-octanol). Obviously, the great variety of $\delta A_{\alpha 1}/A_{\alpha 1}$ values corresponds with the variance in the static dielectric permittivity of alcohol isomers,¹ reflecting a range of different liquid structures.

In view of the significant differences in the behavior of the two groups of alcohols, which are incompletely understood at the present, we shall evaluate the relaxation amplitudes only for a rough estimate of the reaction volume.

Let us assume the low frequency acoustical relaxation to be mainly due to an equilibrium between alcohol monomers A_1 and H-bonded clusters A_p made of p monomers. Solov'ev and Fedotova⁴⁴ analyzed, at some restrictions on the forward and reverse rate constants as well as on the reaction volumes and enthalpies, the isodesmic reaction scheme



with $p = 1, 2, 3, \dots$. Unfortunately, we do not know the size distribution of the clusters and thus the distribution of relaxation rates for the alcohols. For this reason, we estimate an adiabatic reaction volume

$$\Delta V_{ad,1} = \left(\frac{RTA_{\alpha 1}}{\pi \Gamma_1 c_{\infty}^2 \rho} \right)^{1/2} \quad (26)$$

considering the monomer exchange with chainlike alcohol clusters of mean size $p = \mu$:



For this equilibrium

$$\Gamma_1^{-1} = [A_1]^{-1} + [A_{\mu}]^{-1} + [A_{\mu+1}]^{-1} \quad (28)$$

As according to computer simulations, the mean cluster size is small ($\mu \approx 4$) and since the monomer concentration amounts to only one to two percent of the total alcohol concentration,⁴⁵ the stoichiometric factor is predominantly given by $[A_1]$. Reasonable reaction volumes $\Delta V_{ad,1}$ on the order of 10 cm³/mol follow on these assumptions from the acoustical relaxation amplitudes.

High-Frequency Shear Viscosity. Recent frequency dependent shear viscosity measurements of n -alkanes⁶ confirmed previous ideas^{21,23,24} of collective conformational isomerizations of alkyl chains to be accompanied by a shear viscosity relaxation. For the alcohols measured in this study the ultrasonic

absorption spectrum clearly reveals a high-frequency relaxation term due to the formation of alkyl chain rotational isomers. The relaxation frequency $\nu_{\alpha 2}$ of this term, however, is too high to enable a verification by shear impedance spectrometry. Using eq 24 analogously the shear viscosity relaxation amplitude $\eta_s(\infty) - \eta_{s\infty}$ following from the alkyl chain isomerization can be calculated from the acoustical relaxation parameters:

$$\eta_s(\infty) - \eta_{s\infty} = \frac{3A_{\alpha 2}\tau_{\alpha 2}\rho c^2}{4\pi} \quad (29)$$

Here $\eta_s(\infty)$ is the high-frequency shear viscosity as extrapolated from the experimental frequency dependent η_s data (Table 3), whereas $\eta_{s\infty}$ is the high-frequency limiting shear viscosity of the presumed chain isomerization process. Hence $\eta_{s\infty}$ is the viscosity to be used in the discussion of fast molecular dynamics ($\nu > 5\text{GHz}$).

Along with the low-frequency viscosity values, the $\eta_{s\infty}$ data for the monohydric alcohols and for some *n*-alkanes are displayed in Figure 8. Interesting, for both the associating and the nonassociating liquids, quite uniform $\eta_{s\infty}$ values at around 1 mPa s result.

References and Notes

- (1) Crossley, J. *Adv. Mol. Relax Processes*. **1970**, *2*, 69.
- (2) Takagi, Y.; Yano, T.; Mikami, M.; Kojima, S. *Phys. B* **1999**, *263–264*, 306.
- (3) Hoffmann, H.; Löbl, M.; Rehage, H. In *Physics of Amphiphiles: Micelles, Vesicles and Microemulsions*; Degiorgio, V., Corti, M., Eds.; North-Holland: Amsterdam, 1985.
- (4) Dreyfus, C.; Aouadi, A.; Pick, R. M.; Berger, T.; Patkowski, A.; Steffen, W. *Eur. Phys. J. B* **1999**, *9*, 401.
- (5) Fukuda, H.; Kinoshita, S. *J. Lumin.* **2000**, *87–89*, 712.
- (6) Behrends, R.; Kaatze, U. *J. Phys. Chem. A* **2000**, *104*, 3269.
- (7) Herzfeld, K. F.; Litovitz, T. A. *Absorption and Dispersion of Ultrasonic Waves*; Academic Press: New York, 1959.
- (8) Kaatze, U.; Hushcha, T. O.; Eggers, F. *J. Solution Chem.* **2000**, *29*, 299.
- (9) Eggers, F.; Kaatze, U. *Meas. Sci. Technol.* **1996**, *7*, 1.
- (10) Kaatze, U.; Wehrmann, B.; Pottel, R. *J. Phys. E: Sci. Instrum.* **1987**, *20*, 1025.
- (11) Eggers, F.; Kaatze, U.; Richmann, K. H.; Telgmann, T. *Meas. Sci. Technol.* **1994**, *5*, 1131.
- (12) Kaatze, U.; Lautscham, K.; Brai, M. *J. Phys. E: Sci. Instrum.* **1988**, *21*, 98.
- (13) Kaatze, U.; Kühnel, V.; Weiss, G. *Ultrasonics* **1966**, *34*, 51.
- (14) Lamb, J. In *Molecular Basis of Transitions and Relaxations*; Meier, D. J., Ed.; Gordon and Breach: London, 1978.
- (15) Behrends, R.; Kaatze, U. *Meas. Sci. Technol.* **2001**, *12*, 519.
- (16) Kaatze, U.; Kühnel, V.; Menzel, K.; Schwerdtfeger, S. *Meas. Sci. Technol.* **1993**, *4*, 1257.
- (17) Marquardt, D. W. *J. Soc. Ind. Appl. Math.* **1963**, *2*, 2.
- (18) Cole, K. S.; Cole, R. H. *J. Chem. Phys.* **1941**, *9*, 341.
- (19) Debye, P. *Polar Molecules*; Chemical Catalog: New York, 1929.
- (20) Behrends, R. Dissertation, Georg-August-Universität Göttingen, Göttingen, 1999.
- (21) Tobolsky, A. V. *J. Polym. Sci. A-2* **1968**, *6*, 1177.
- (22) Tobolsky, A. V.; DuPré, D. B. *Adv. Polym. Sci.* **1969**, *6*, 103.
- (23) Cochran, M. A.; Jones, P. B.; North, A. M.; Pethrick, R. A. *J. Chem. Soc., Faraday Trans. 2* **1972**, *68*, 1719.
- (24) Pitzer, K. S. *J. Chem. Phys.* **1944**, *12*, 310.
- (25) Träuble, H.; Haynes, D. *Chem. Phys. Lipids* **1971**, *7*, 324.
- (26) Barthel, J.; Bachhuber, K.; Buchner, R.; Hetzenauer, H. *Chem. Phys. Lett.* **1990**, *165*, 369.
- (27) Buchner, R.; Barthel, J. *J. Mol. Liq.* **1992**, *52*, 131.
- (28) Richards, M. G. M. Dissertation, King's College London, London, 1993.
- (29) Davidson, D. W.; Cole, R. H. *J. Chem. Phys.* **1950**, *18*, 1417.
- (30) Jorgensen, W. L. *J. Chem. Phys.* **1986**, *90*, 1276.
- (31) Petong, P.; Pottel, R.; Kaatze, U. *J. Phys. Chem. A* **1999**, *103*, 6114.
- (32) Petong, P.; Pottel, R.; Kaatze, U. *J. Phys. Chem. A* **2000**, *104*, 7420.
- (33) Debus, A. Diploma-Thesis, Georg-August-Universität Göttingen, Göttingen, 1996.
- (34) Padró, J. A.; Saiz, L.; Guàrdia, E. *J. Mol. Struct.* **1997**, *416*, 243.
- (35) Saiz, L.; Padró, J. A.; Guàrdia, E. *J. Phys. Chem. B* **1997**, *101*, 78.
- (36) Sagal, M. W. *J. Chem. Phys.* **1962**, *36*, 2437.
- (37) Geiger, A.; Mausbach, P.; Schnitker, A. In *Water and Aqueous Solutions*; Neilson, G. W., Enderby, J. E., Eds.; Hilger: Bristol, 1986; p 15.
- (38) Tanaka, H.; Ohmine, I. *J. Chem. Phys.* **1987**, *87*, 6128.
- (39) Sciortino, F.; Geiger, A.; Stanley, H. E. *J. Chem. Phys.* **1992**, *96*, 3857.
- (40) Ohmine, I.; Tanaka, H.; Wolynes, P. G. *J. Chem. Phys.* **1998**, *89*, 5852.
- (41) Gestblom, B.; El-Samaky, A.; Sjöblom, J. *J. Sol. Chem.* **1985**, *14*, 375.
- (42) Schwerdtfeger, S.; Dissertation, Georg-August-Universität Göttingen, Göttingen, 1996.
- (43) Kaatze, U.; Behrends, R.; Pottel, R. *J. Non-Cryst. Solids*, in press.
- (44) Solov'ev, V. A.; Fedotova, S. Y. *Acoust. Phys.* **1994**, *41*, 5.
- (45) Jorgensen, W. L. *J. Chem. Phys.* **1986**, *90*, 1276.